Validation of MBS modeling methods to calculate bearing and tooth loads in the planetary gear stage of a wind turbine

Daniel Matzke[*1],
Ralf Schelenz, Georg Jacobs[1]

[1]Center for Wind Power Drives
Campus-Boulevard 61, 52074 Aachen, Deutschland

Contents

1 Motivation

Due to the increasing cost pressure, a reliable wind turbine (WT) is a major priority. Reliability is strongly determined by the design process. Therefore, it is important to have accurate and reliable load assumptions, ideally at early stages of the design process. Yet, due to the high dynamic loads in all six degrees of freedom (DOF) that a rotor couples into the drive system and the influence of the electric system and controller, load calculation for WT and their components is challenging. Thus, to improve the design process and the reliability of WTs and their components, simulation models are needed that can robustly calculate loads while taking system wide interdependencies into account. Therefore, entire system models are developed and validated at the Center for Wind Power Drives (CWD) [BER16][MAT18].

This contribution discusses the potential of entire system simulations based on detailed multi-body simulation (MBS) models to improve the design process. Furthermore the validation of the load calculation of a full scale wind turbine MBS model is presented. The modelled wind turbine is the “FVA-Gondel”, a 2.75 MW generic research wind turbine. The loads calculated with the MBS model are compared with comprehensive load measurements from a full scale 4 MW system test bench [LIE17]. System test benches for wind turbine nacelles present an efficient tool for model validation. It is possible to test system behavior and repeatedly and reproducibly measure loads under controlled conditions. At the CWD, a 4 MW system test bench is operated with the “FVA-Gondel” as device under test (DUT). A Hardware-in-the-loop (HIL) system is used to calculate aerodynamic loads and emulate inertia, dynamic behavior of the rotor as well as grid loads to account for realistic system behavior [LIE15][WEL14][AVE15].

With respect to the levelized cost of energy the gearbox is one of the most critical components, due to long downtimes and expensive repairs in case of failure [SHE16]. Literature suggests that some of the most common or costly failures of gears and bearings result from certain load states not taken into consideration during the design process [LIN11]. This contribution focuses on the dynamic load state time series calculation of the gearbox and its subcomponents, i.e. gear and bearing loads and load distributions, in an entire system simulation under realistic operation conditions. It is evaluated which model parameters influence these calculation objectives as well as the modelling methods and fidelity required to represent them meaningfully. To maintain a meaningful scope, only the validation of the bearing and tooth loads of the first gear stage, a planetary gear stage, is considered in this paper.

2 Outline

Some of the most crucial design relevant loads of the gearbox components are the tooth loads as well as bearing loads in the first planetary gear stage. These depend on local

microgeometry and contact conditions as well as global deformations caused by the above discussed high loads in addition to complex system wide interdependencies. Therefore, an entire system model of the turbine on the test bench with a detailed MBS model of the drive train and especially the gearbox is set up to calculate dynamic tooth and bearing loads [MAT17]. Then, a comparison of the calculation results with extensive load measurements is presented to show the validity of the model and its capabilities. The method to obtain the load measurements was previously presented and is not discussed in this paper [LIE17]. The results are used to develop suitable modelling strategies and analyze their potential for improving the design process.

The following section gives an overview on the state of the art of wind turbine gearbox load calculation and design. The presented work is put into perspective of current international research with respect to these topics. Then, the setup of the models is discussed in section 4. In section 5, the validation of the bearing and tooth load calculation with the model is presented and discussed in-depth. A discussion of the devised model strategies and modelling method improvements is conducted subsequently. Finally, a conclusion and an outlook are given.

3 State of the art

The current state of the art of WT gearbox design mostly consists of modification and redesign of existing type series and subsequent field testing. Furthermore, design deficiencies are approached by re-engineering deficient components, replacing them in the turbine and testing them in the field. This process is costly and while it leads to a better design, turbine reliability is not improved in a fast matter. During the preliminary design as well as during the detailed component design, simulation models are used for load calculation. However, these are mostly simple gear load calculation tools like RIKOR or LVR, which factor in the discussed load conditions of a WT only on a minimal level. Furthermore, if more advanced simulation tools are used, typical state of the art model fidelity as advised by the IEC [VDE11] or GL [GL03] for models for the design or certification process are rather low. The authors believe that MBS-based entire system simulations can provide more reliable and more detailed load calculations and therefore improve the design process and the reliability of turbines significantly. This is a problem the industry begins to acknowledge, recognizable by the content of the last guidelines and recommendations of the DNV GL [BOC15] or current research of Nalliboyana et al. (Winergy) [NAL17].

Consequently, the international research community has taken on the task of researching load states in gearboxes and developing improved drive train simulation methods. There is a lot of research being conducted with respect to more detailed MBS models of WT drive trains [SCH17] or the setup of system test benches for gearbox reliability research and model validation [SCH16][ZHA17]. Nonetheless the Gearbox Reliability Collaborative (GRC) of NREL is the only other contribution that combines systematic anal-

yses of load states and load calculation in a wind turbine gearbox under realistic reproducible torque and non-torque loads combined [LIN11]. GRC was able to show the importance of non-torque loads on gear tooth load distribution, importance of model fidelity (e.g. representation of the bearing clearance and assembly variations) and representation of the flexibility of the planet carrier and gearbox housing [LIN11].

4 Model

The model topology of the developed entire system simulation is shown in **Fehler! Verweisquelle konnte nicht gefunden werden.**. Main part of the model is the mechanical MBS model of the turbine on the test bench. This is connected to a model of the HiL-system of the test bench as well as electromagnetic transient (EMT) models of the electrical system in Simulink via co-simulation. The EMT-models consist of a generator, a converter and a grid model. Furthermore the model of the original controller of the turbine is used to operate the model. The modeling methods and model fidelity of the Simulink-models have already been presented in previous works of the authors [MAT17] and will not be discussed in this paper. The following paragraphs will only contain a presentation of the MBS model.

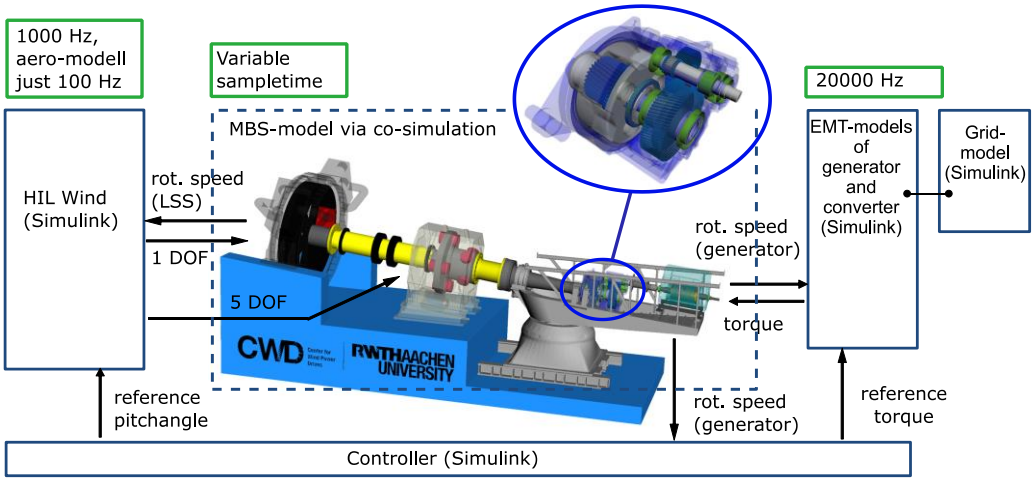

Figure 1: Topology of the entire system simulation with a graphical representation of the MBS model

A MBS model in 6 DOF of the turbine on the test bench with a detailed gearbox model as shown in **Fehler! Verweisquelle konnte nicht gefunden werden.** is set up. For all shafts and the planet carrier as well as structural components FE models have been set up to calculate the stiffness characteristics. The models of the components that show relevant deformation under load are modally reduced using the Craig-Bampton method [CRA68] and then implemented as flexible bodies in the model. Those are the shafts of the drive train, the main frame and tower adapter as well as planet carrier and gearbox housing.

The stiffness characteristic of the bench's geared coupling is calculated by FE. The stiffness behavior is implemented as spring-damper element. For the steel disk coupling between gearbox and generator manufacturer data is used and implemented as force element. The stiffness and damping behavior of the elastomer mountings of the generator have been measured on a linear cylinder test bench and are implemented as force elements. The stiffness and damping characteristics of the elastomer bushings of the torque arms have been measured by the manufacturer and are implemented as force elements as well.

All gears are modeled using a force element which calculates the forces analytically based on linear material deformation. The calculation of the stiffness characteristic is done according to the DIN 3990. The stiffness behavior of the bearings was calculated based on manufacturer data and is implemented as force elements representing the non-linear stiffness characteristics including clearance. An exception is the yaw bearing for which an FE model has been set up to calculate the highly non-linear stiffness characteristic based on the loading situation.

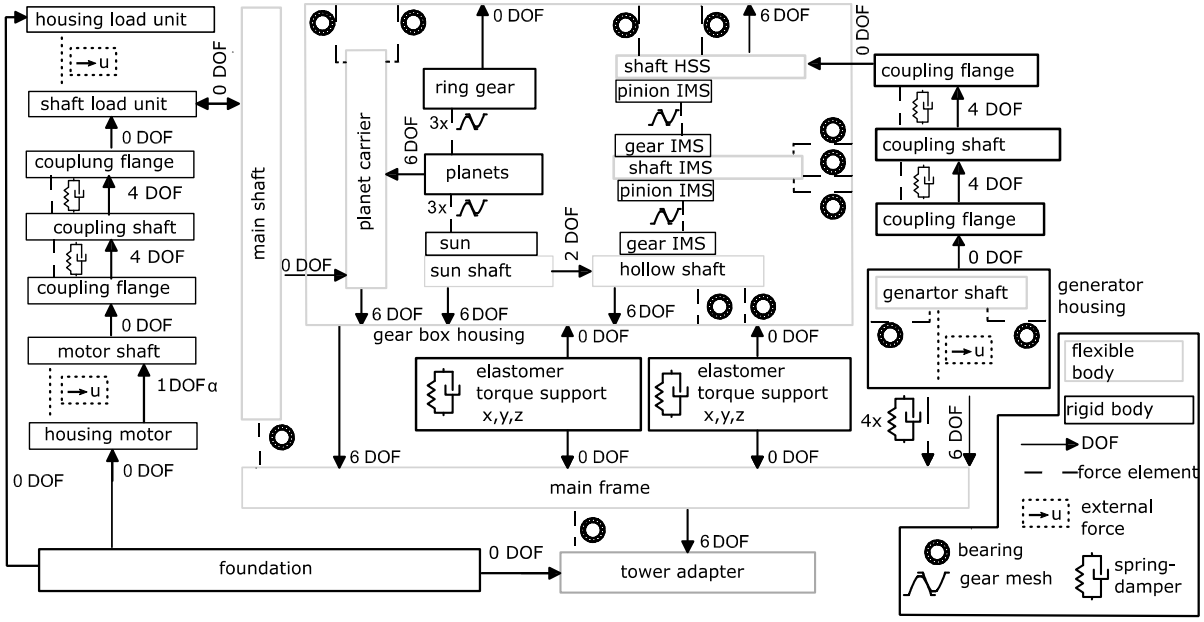

Figure 1: Topology of the MBS model of the turbine on the test bench including the detailed gearbox model

5 Validation Results

This section starts with representative validation results for the entire system behavior of the model. The next subsection focuses on the detailed gear and bearing load calculation of the MBS model alone, showing the validation of the model for different stationary load conditions for the turbine. The third subsection shows an excerpt of the load calculation of the model for turbulent wind conditions in power production mode. Then, this is used to discuss the suitability of the model to calculate lifetime load spectra. A

fourth part presents results for a new approach to take the flexibility of the gear bodies into consideration and discusses its potential for the load calculation.

5.1 Entire System simulation

To show the validity of the entire system simulation, a wind field with 14 % turbulence intensity and increasing mean wind speed (see Figure 2) is applied on the HiL-model of the turbine on the test bench as well as on the entire system model. **Figure 3** shows the values for the pitch angle that the controller of the turbine applies. **Figure 4** and **Figure 5** show the resulting rotational speed and the applied generator torque, according to the characteristic curve. It can be seen that for the first 200 seconds, the turbine runs in partial load operation. The pitch is at 0° while the rotational speed and torque follow the mean wind. At around 14 m/s the turbine switches to full load operation mode. The pitch controller is then active and keeps rotational speed and torque at nominal value. Except for deviations at the transition between partial and full load, which is due to a slightly different supervisory control model, the model matches the behavior of the turbine on the test bench. For more information regarding the HiL-model and test bench, see [LIE15][WEL14][AVE15].

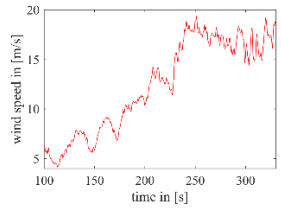

Figure 2: Hub height wind speed of turbulent wind field (increasing mean wind speed; 14% turbulence intensity)

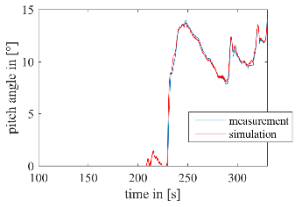

Figure 3: Pitch angle

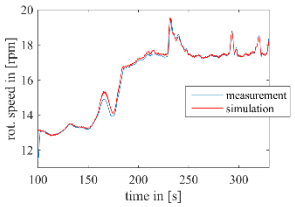

Figure 4: Rotational speed of Low-Speed-Shaft (LSS)

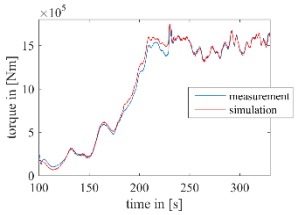

Figure 5: LSS torque

5.2 MBS model of the turbine (including the detailed gearbox model)

In this subsection the validity of the MBS model regarding the planet bearing load calculation for different stationary load conditions is shown. These bearings consist of two cylindrical roller bearings with two rows of rollers each. The naming convention used in this paper is shown in **Figure 6**. In **Figure 7** a comparison between the load calculation of the model and test bench measurements for each row can be seen. The development of values of the model matches the measurements quite well. Especially the once per rotation oscillation of the four rows, thus a varying load distribution between the bearings every 5.5 seconds, is matched. The cause of this effect is discussed below, when the gear loads are also considered as well. An exception poses the third row. This row shows lower loads than expected throughout every measurement done so far [LIE17], which leads to the assumption of a measurement issue or an unusually larger clearance.

Figure 8 shows the development of values for a reduced torque. The match between simulation and measurement is as good as previously, with the loads being a little lower as would be expected. In **Figure 9** the loads for a variation of the tilt-bending can be seen. This moment has a rather large influence on the loads of the first gear stage, which has been validated and explained in previous works of the authors [MAT18-2]. The model represents this behavior. As can be seen in **Figure 10**, a variation of the yaw-bending has a much lower influence, just slightly decreasing the amplitude of the oscillation. The model also represents this effect correctly.

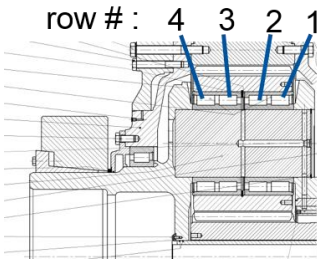

Figure 6: The 4 rows of the planetary bearings

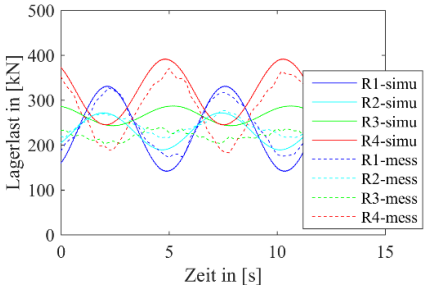

Figure 7: Loads of all rows at reference load case

Table 1: Reference load case:

Torque	1500	kNm
Thrust	0	kN
Shear force (rotor weight)	-488	kN
Tilt-bending	0	kNm
Yaw-bending	0	kNm
Rotational speed	11	rpm

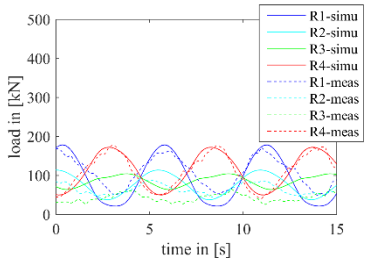

Figure 8: Loads of all rows at a reduction of the torque to 500 kNm

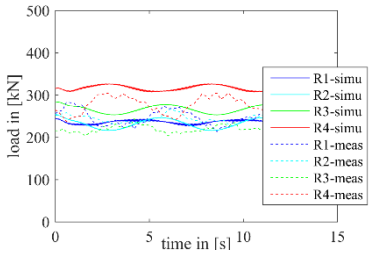

Figure 9: Loads of all rows at a reduction of the tilt-bending to -1500 kNm

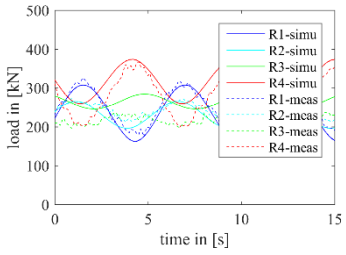

Figure 10: Loads of all rows at an increase of the yaw-bending to 1000 kNm

Figure 11 to **Figure 14** show the tooth load distributions of the planet-sun and planet-ring gear meshes for the reference load case. This can only be done for isolated points in time, since only four teeth of the ring gear are equipped with strain gauges to measure the loads [LIE17]. They are at 0, 90, 180 and 270 degree, the numbering being counted from 0 at the top while looking from the rotor side. The bearing loads are also plotted into the graphs, being scaled width related. First of all it can be seen, that the once per rotation occurring uneven load distribution of course also affects the tooth loads. The figures show that the bearing load distribution and the tooth load distribution counterbalance each other. It can also be seen that the worst distribution is at 90 degrees. This is due to a large flank line deviation. The deviation is caused by a misalignment of the planet carrier due to the clearance of its bearings [MAT18-2] and torsion of the planet carrier both reinforcing this effect at this position. This causes the uneven load distribution of the teeth, which then results in the uneven load distribution of the bearings that are counterbalancing these loads. It can be seen that the model matches not only the

bearing load distribution, as has been shown previously, but also the tooth load distribution, representing the discussed effects.

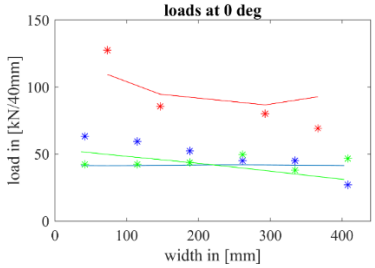

Figure 11: Axial load distribution of the planets gears and bearings (Planet at 0 deg)

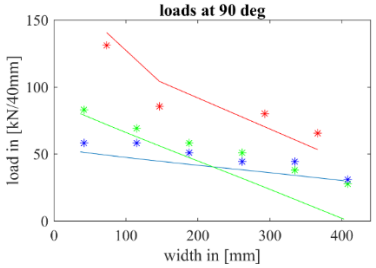

Figure 12: Axial load distribution of the planets gears and bearings (Planet at 90 deg)

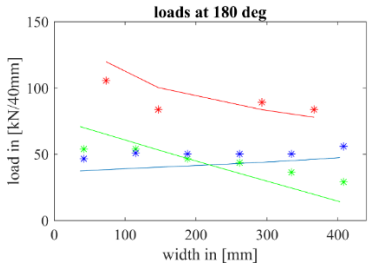

Figure 13: Axial load distribution of the planets gears and bearings (Planet at 180 deg)

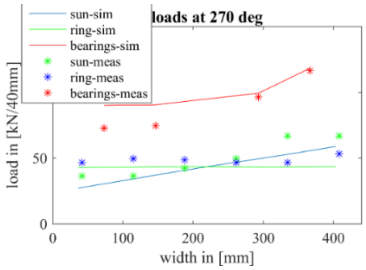

Figure 14: Axial load distribution of the planets gears and bearings (Planet at 270 deg)

To achieve these results, a gearbox model as detailed as described in the model section is necessary. Especially the planets and the planet carrier need to have 6 DOF and the bearing stiffness characteristics need to be represented properly including clearance. The stiffness of the planet carrier also has a significant influence. These findings correspond with the initially discussed findings of GRC [LIN11] and can easily be explained by analyzing the cause of the above discussed flank line deviation. Furthermore the modelling of all four bearing rows is necessary. The stiffness characteristics of the gearbox housing, the main shaft as well as the elastomer bushings or the torque arms also have a large influence and need to be represented accordingly. The main frame has some, but not much influence on these loads.

5.3 Lifetime load calculation

The combination of the entire system simulation with the detailed MBS-model allow calculation of the machine elements loads for arbitrary wind fields.

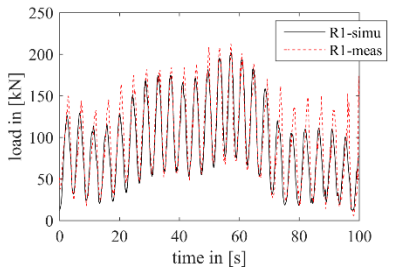

Figure 15: Planet bearing load of row 1 for model and measurement for a mean wind speed of 8 m/s with 12 % turbulence

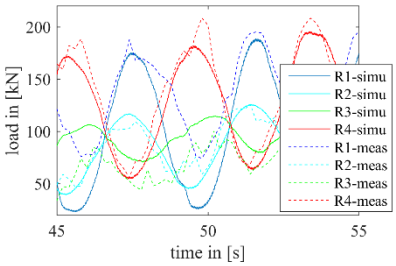

Figure 16: Excerpt of bearing loads for all rows for model and measurement for the same wind field as in Figure 15:

Figure 15 shows the development of values for row 1 of the planet bearings for a turbulent wind field of 100 seconds. The comparison between simulation and measurement shows good results, with slight deviations at very low loads. In **Figure 16** an excerpt of the very same simulation is shown for all four rows, yet only for 10 seconds, for clarity of the diagrams. These results can then be used to calculate dynamically equivalent bearing loads for all rows and for arbitrary wind conditions, as is done for an exemplary wind field in **Figure 17**. Except for row 3, which deviates as discussed earlier, the calculated values match the measured ones quite well. To evaluate the models potential to improve the design process, the same simulations are carried out with models according to the minimal necessary recommendations of the IEC [VDE11] and GL [GL03]. **Figure 18** shows that the developed model achieves a better match with the measurements than these models.

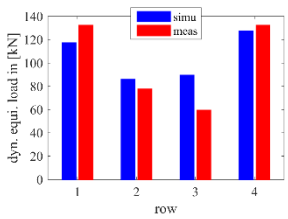

Figure 17: Dynamically equivalent bearing loads for row 1-4 for model and measurement for a 200 seconds wind field

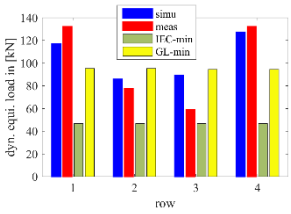

Figure 18: Comparison of dynamically equivalent bearing loads for the model and models as advised by IEC or GL

5.4 Flexible planets

The so far discussed loads are needed for the service life time calculation of the bearings. Yet, a contact stress calculation is part of the design process as well and a better knowledge of the contact stress can help understand the effects on the bearing fatigue. Therefore more detailed calculations of the load distribution, also in circumferential direction is needed. For that, the circumferential load distribution is measured for each row at 3 different positions, as is visualized in Figure 19 [LIE17]. Yet, the presented model as well as other models set up during the project, for example a model with the FVA workbench [LIE17], cannot match the circumferential load distribution. The loads in the middle of the load zone are always overestimated by the models and the width of the

load zone was underestimated. Liewen found that this is due to the neglect of the planets bodies ovalization [LIE17]. Therefore a MBS model is set up with flexible planet gear bodies. While the gear body is represented by a modally reduced FE body, the tooth deformation and contact stiffness are still calculated according to DIN 3990 by the used method and applied locally on the flexible body. Figure 20 shows a graphical visualization of the results. The ovalization can be seen due to a upscaling of the deformation, as well as the discussed decrease of the loading in the middle of the load zone as well as the widening of the load zone. **Figure 21** to **Figure 24** show the numeric results for each row at reference load and the planet being at 90 degree. The model with the flexible planet bodies obtains a way better result, both in numeric value as in characteristic of the distribution. This effect is achieved for all positions of the planet and load conditions.

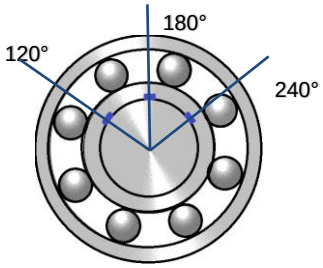

Figure 19: Positions of strain gauges in inner ring

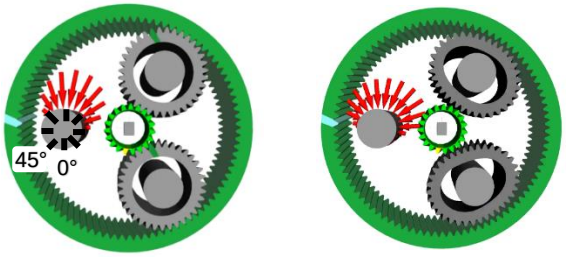

Figure 20: Circumferential load distribution with rigid and flexible planet bodies

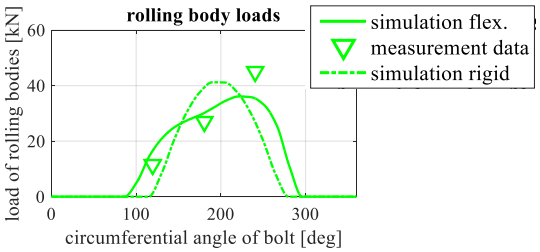

Figure 21: load distribution for row 4

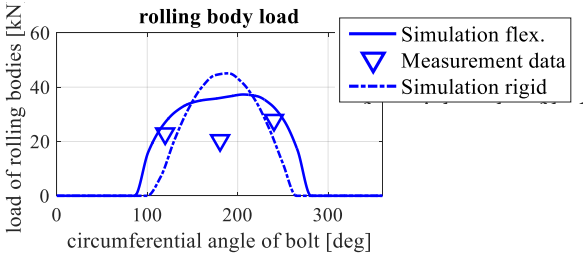

Figure 22: load distribution for row 3

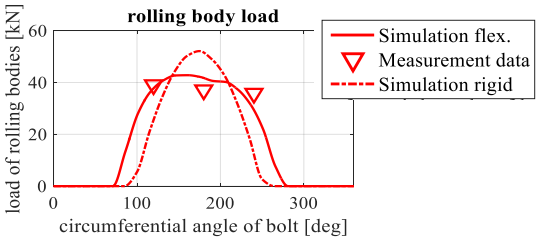

Figure 23: load distribution for row 2

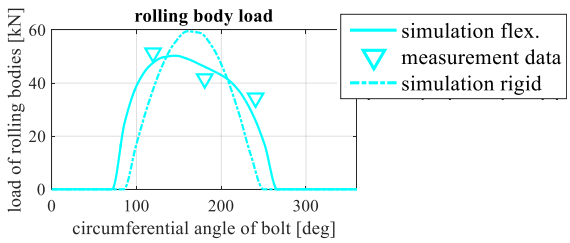

Figure 24: load distribution for row 1

6 Summary and outlook

The authors believe that entire system simulations based on detailed MBS models can help improve the design process of wind turbines. Therefore such a model is set up and load calculation results are compared to test bench measurements under realistic load conditions, to validate the model and improve modelling strategies. The relevant model

parameters are evaluated by the authors, the most relevant being the bearings stiffness characteristics and clearance, the stiffness of the planet carrier as well as the representation of all four planet bearing rows. The design relevant loads are then compared to state of the art calculation methods to evaluate the potential of the devised model. It could be shown that the model provides more accurate results.

Future work will focus on the calculation of lifetime equivalent bearing loads considering life-time load spectra by taking into account the IEC wind classes. Also the design relevant loads of the gears for these load spectra will be calculated and compared to the state of the art design process. Furthermore, model reductions will be researched to make the approach more suitable for industry.

7 Bibliography

[MAT18] D. Matzke et al.: Multi-body-Simulation in wind energy – From turbine design to detailed component load calculation.

4th Wind And Drivetrain Conference, 2018

[BER16] J. Berroth et al.: Nacelle Test Benches for Model Validation Simpack Wind and Drive Train Conference, 2015.

[LIE17] C. Liewen et al.: Validation of planetary bearing loads in wind turbine gearboxes on a 4 MW system test bench

Conference for Wind Power Drives 2017, Aachen

[LIE15] C. Liewen et al.: New infrastructure and test procedures for analyzing the effects of wind and grid loads on the local loads of wind turbine drivetrain components

Proceedings of DEWEK 2015, 19/20 May 2015

[WEL14] S. Wellenberg et al.: Real-time simulation of aeroelastic rotor loads for horizontal axis wind turbines

The Science of Making Torque from Wind 2014

[AVE15] N. Averous et al.: Development of a 4 MW Full-Size Wind-Turbine Test Bench

2015 IEEE 6th International Symposium on Power Electronics for Distributed Generation Systems

[SHE16] S. Sheng, Wind Turine Gearbox Reliability Database, Condition Monitoring, and Operation and Maintenance Research Update

NREL Report NREL/PR-5000-66028, 2016

[LIN11] H. Link et al.: Gearbox Reliability Collaborative Project Report: Findings from Phase 1 and Phase 2 Testing

Technical Report, NREL/TP-5000-51885, June 2011

[MAT17] D. Matzke et al.: Full scale system simulation of a 2.7 MW wind turbine on a system test bench

Conference for Wind Power Drives 2017, Aachen

[VDE11] VDE: DIN EN 64100-1

2011

[GL03] Germanischer Llyod WindEnergie GmbH: Richtlinien für die Zertifizierung von Windkraftanlagen I-IV

Hamburg 1993 bis 2003

[BOC15] A. Bockstedte: Evaluation of the minimum requirements for the dynamic analysis of wind turbine drive trains from the certification point of view Technical Report

In: Conference for Wind Power Drives, Aachen (Germany), 2015

[NAL17] D. Nalliboyana1 et al.: A systematic approach for optimizing planetary gear sets for low vibrations

Conference for Wind Power Drives 2017, Aachen

[SCH17] *B. Schlecht* et al.: Possibilities and limitations of the load determination for wind turbines using the multibody-system simulation

Conference for Wind Power Drives 2017, Aachen

[SCH16] R. Schkoda, Virtual Testing of Full Scale Wind Turbine Nacelles

Simpack News February 2016

[ZHA17] H. Zhang et al.: Mechanical Torque Measurement of a Wind Turbine Drive Train under Test on the Nacelle Test Bench Dynalab

DEWEK 2017

[CRA68] Craig, R. R. Jr., Bampton,M. C. C: Coupling of Substructures for Dynamic Analysis

In: AIAA Journal, Vol. 6, No. 7, 1968, pp. 1313-1319

[MAT18-2] D. Matzke et al.: Validation of the gearbox load calculation of a wind turbine MBS model

The Science of Making Torque from Wind 2018